Available online at www.sciencedirect.com
SCIENCE DIRECT
ELSEVIER
Journal of the European Ceramic Society 26 (2006) 2973–2978
ECERS
www.elsevier.com/locate/jeurceramsoc

Misorientation characteristics of interphase boundaries in particulate Al_2O_3-based composites

K. Sztwiertnia [a,*], M. Faryna [a,b], G. Sawina [a]

[a] *Polish Academy of Sciences, Institute of Metallurgy and Materials Science, 25 Reymonta St., 30-059 Krakow, Poland*
[b] *Jagiellonian University, Regional Laboratory of Physicochemical Analyses and Structural Research, 3 Ingardena St., 30-60 Krakow, Poland*

Abstract

It is well known that the character and distribution of interphase boundaries has a significant impact on the properties of polycrystalline materials. For the quantitative characterization of interfaces between matrix and inclusions in two composite systems (Al_2O_3/WC and Al_2O_3/W), large sets of crystallographic misorientation data has been used. The misorientations were measured between the neighbouring regions of different phases. The experiment was based on orientation maps obtained by Electron BackScatter Diffraction (EBSD) in an Environmental Scanning Electron Microscope (ESEM). For the particular arrangements of crystallite symmetries, Misorientation Distribution Functions (MDF) have been developed in such a way that each physically distinct misorientation was represented only once. Preferences for the special crystallographic correlations between matrix grains and inclusions, as well as the shares of interphase boundaries characterized by those correlations, have been evaluated in both composites.

Keywords: Electron microscopy; Interfaces; Al_2O_3; Misorientations

1. Introduction

Several properties of materials depend, to a large extent, on the character of the grain and interphase boundaries. Such a relationship is particularly important in the case of composites, where the strength of the interphase boundaries between matrix grains and inclusions has a crucial impact on the mechanical properties of the polycrystalline sintered bodies (e.g.[1,2]). Due to the development of Orientation Mapping (OM) techniques, both in Scanning Electron Microscope (SEM) (e.g.[3]) and in Transmission Electron Microscope (TEM) (e.g.[4]), a more precise quantitative characterization of boundaries in larger volumes of material becomes possible. At present, the progress in the automation of diffraction measurements allows the EBSD in the SEM to be used extensively to create orientation maps.

This work presents two examples of analysis of particulate composites with an alumina matrix and tungsten carbide or tungsten additive (the composite systems: Al_2O_3/WC and Al_2O_3/W) to show that the measurements of orientation topography enables the quantitatively evaluation of the crystallographic relationships between grains of different phases. The research was based on the measurement of orientation maps with the EBSD technique in an ESEM.[a] A quantitative description of crystallographic relationships was obtained from the distributions of misorientation, calculated from the sets of orientation pairs measured in neighbouring sample areas that belong to different phases.

2. Experimental

Composite powders were prepared from commercial powders of alumina (Nabaltec), plus WC and W (Baildonit). The amount of additive was 10% by volume in both cases. The mean grain size of WC powder was 2.5 μm and the W powder about

[a] ESEM permits the manipulation of sample environments by varying pressures and gas compositions in a selected range. Gas ionization during the work with low vacuum in the sample chamber eliminates charging artifacts, typically seen with nonconductive samples (e.g. Al_2O_3-based composites). It enables easy examination of such samples in their natural state (i.e. without modification of their surface).

* Corresponding author. Tel.: +48 12 637 4200; fax: +48 12 637 2192.
E-mail address: nmsztwie@imim-pan.krakow.pl (K. Sztwiertnia).

0955-2219/$ – see front matter © 2006 Published by Elsevier Ltd.
doi:10.1016/j.jeurceramsoc.2006.02.014

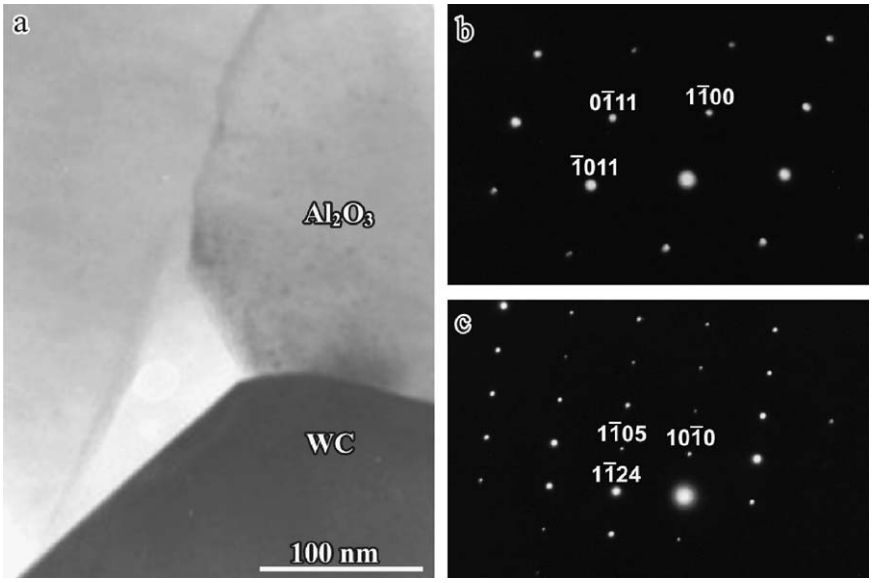

Fig. 1. Microstructure of Al_2O_3/WC composite, obtained by TEM. (a) Bright field image; (b) SAED from WC grain; (c) SAED from Al_2O_3 grain.

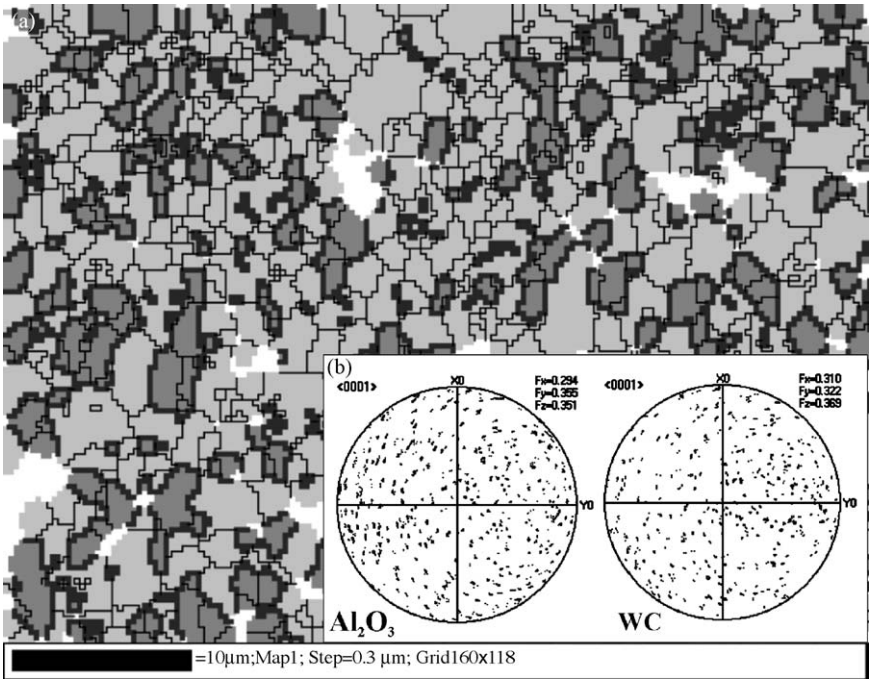

Fig. 2. Microstructure of Al_2O_3/WC composite. (a) ESEM/EBSD orientation map; Al_2O_3 grains: light grey; WC grains: dark grey; white regions: not indexed; thick lines: Al_2O_3/WC interphase boundaries, thin lines: grain boundaries. (b) Stereographic projections of directions $\langle 0\,0\,0\,1\rangle$ for Al_2O_3 grains and WC grains, respectively; the measurement field is that shown in (a).

2 μm. The composite powders were homogenised in an attritor mill in ethyl alcohol. Sintering of samples was conducted using a hot-pressing technique.[2] The composite microstructures were examined using Selected Area Electron Diffraction (SAED), in the TEM, and ESEM/EBSD techniques.

2.1. Example I, composite Al_2O_3/WC

By use of TEM/SAED (Fig. 1),[6] the following crystallographic relationships between WC inclusions with hexagonal (D_6) crystal lattice symmetry and grains of Al_2O_3 matrix with trigonal (D_3)[b] crystal lattice symmetry have been determined:

$$(0\,\bar{1}\,1\,1)\mathrm{WC}\|(\bar{1}\,0\,1\,1)\mathrm{Al_2O_3}\quad (0\,\bar{1}\,1\,1)\mathrm{WC}\|(1\,\bar{1}\,0\,5)\mathrm{Al_2O_3}$$
$$[2\,\bar{1}\,\bar{1}\,0]\mathrm{WC}\|[0\,1\,\bar{1}\,1]\mathrm{Al_2O_3}\,,\quad [1\,1\,\bar{2}\,3]\mathrm{WC}\|[\bar{2}\,3\,\bar{1}\,1]\mathrm{Al_2O_3}$$

[b] Al_2O_3 is of trigonal symmetry. We use, however, the Miller–Bravais notation when describing planes and directions in Al_2O_3, since the pseudo-hexagonal oxygen sublattice dominates most crystallography-determined properties (e.g.[5]).

Then, the orientational relationships between Al_2O_3 and WC were examined on large areas by means of the EBSD/ESEM technique. Orientation maps were determined with 0.3 μm measurement steps in five different areas, each 60 by 44 μm. Fig. 2a presents one such map covering both the oxide and carbide phase. Fig. 2b shows the distributions of ⟨0 0 0 1⟩ directions in Al_2O_3 and in WC, respectively. It can be noted that the textures of both phases in the measurement field are approximately random. However, the MDF calculated from about 11000 pairs of grains, inclusion-matrix, is not random and clear maxima in positions: (a) $r_1 = 0.2$, $r_2 = 0.1$, $r_3 = -0.0107$; (b) $r_1 = 0.5$, $r_2 = 0.3$, $r_3 = -0.0107$; (c) $r_1 = 0.0$, $r_2 = 0.0$, $r_3 = -0.2679$; (d) $r_1 = 0.9$, $r_2 = 0.0$, $r_3 = -0.0107$; (e) $r_1 = 0.7$, $r_2 = 0.1$, $r_3 = -0.0107$ can be distinguished (Fig. 3). These maxima can be approximated by the following low-indexed crystallographic relationships:

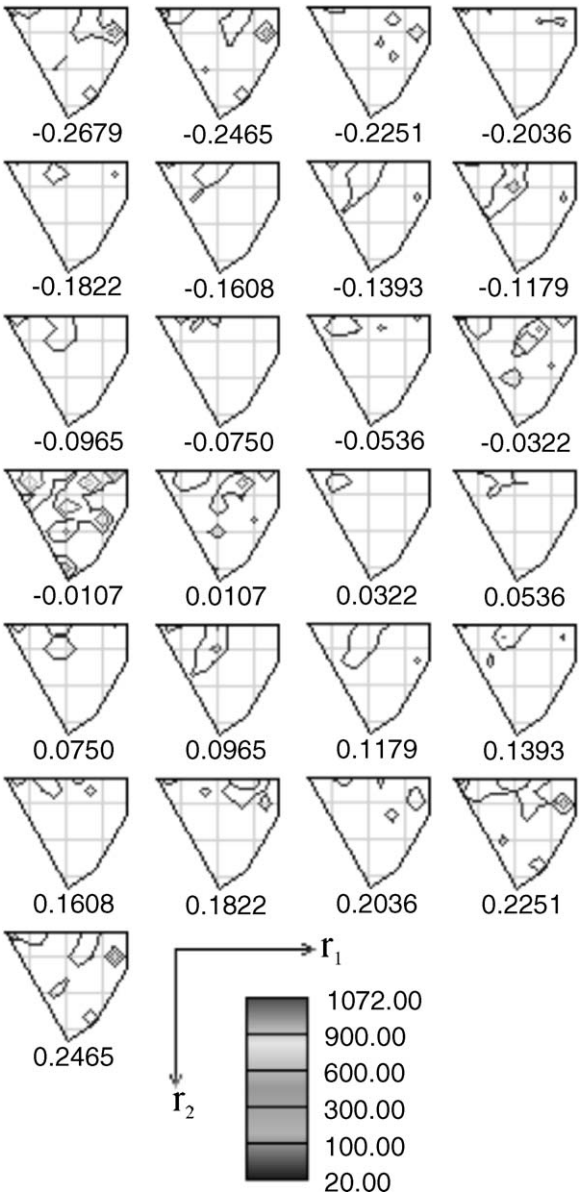

Fig. 3. Misorientation Distribution Function between Al_2O_3 and WC grains; Rodrigues' representation $r_1 \in [0,1]$, $r_2 \in [0,1]$, $r_3 \in [-0.2679, 0.2465]$, cross-section $r_3 = \text{const.}$, asymmetric domain (D_6, D_3).

(a) $(1\,0\,\bar{1}\,0)\mathrm{WC} \| (1\,0\,\bar{1}\,0)\mathrm{Al_2O_3}$, $[0\,0\,0\,\bar{1}]\mathrm{WC} \| [\bar{1}\,3\,\bar{2}\,\bar{2}]\mathrm{Al_2O_3}$

(b) $(1\,0\,\bar{1}\,0)\mathrm{WC} \| (1\,0\,\bar{1}\,0)\mathrm{Al_2O_3}$, $[0\,0\,0\,\bar{1}]\mathrm{WC} \| [\bar{4}\,9\,\bar{5}\,2]\mathrm{Al_2O_3}$

(c) $(0\,0\,0\,1)\mathrm{WC} \| (0\,0\,0\,1)\mathrm{Al_2O_3}$, $[1\,1\,\bar{2}\,0]\mathrm{WC} \| [1\,0\,\bar{1}\,0]\mathrm{Al_2O_3}$

(d) $(2\,\bar{1}\,\bar{1}\,0)\mathrm{WC} \| (2\,\bar{1}\,\bar{1}\,0)\mathrm{Al_2O_3}$, $[0\,0\,0\,\bar{1}]\mathrm{WC} \| [0\,1\,\bar{1}\,0]\mathrm{Al_2O_3}$

(e) $(3\,\bar{1}\,\bar{2}\,0)\mathrm{WC} \| (3\,\bar{1}\,\bar{2}\,0)\mathrm{Al_2O_3}$, $[0\,1\,\bar{1}\,\bar{1}\,2]\mathrm{WC} \| [\bar{1}\,9\,\bar{8}\,\bar{1}]\mathrm{Al_2O_3}$.

The same orientation relationships have been established in the MDF values calculated for the other measurement areas. Assuming that the acceptable deviation of the measured crystallographic directions from the ideal position is smaller than 3°, the above relationships correspond to: 5–8% for (a); 1.5–2% for (b); 7–12% for (c); 6–15% for (d) and 2.5–6% for (e) of the total WC/Al_2O_3 interphase boundary length, depending on the measurement field. The crystallographic relationships between WC and Al_2O_3 identified by means of TEM are located in the range of uncertainty around the positions found by ESEM/EBSD.

2.2. Example II, composite Al_2O_3/W

Similar analysis as in the case of Al_2O_3/WC was performed for the Al_2O_3/W composite. Using TEM/SAED, the following crystallographic relationship between tungsten inclusions with cubic (T_d) crystal lattice symmetry and grains of the alumina matrix has been found (Fig. 4):

$$(2\,\bar{1}\,\bar{1})\mathrm{W} \| (\bar{2}\,4\,\bar{2}\,0)\mathrm{Al_2O_3}$$
$$[1\,1\,1]\mathrm{W} \| [0\,0\,0\,1]\mathrm{Al_2O_3}.$$

Orientation maps were again measured with 0.3 μm steps in three different measurement areas, each 48 by 35 μm. Fig. 5a shows an example of the topography of alumina and tungsten grains. Fig. 5b presents the distributions of ⟨0 0 0 1⟩ directions in Al_2O_3 and of ⟨0 0 0 1⟩ directions in W, respectively. In this case, the textures of both phases are approximately random, contrary to the MDF values calculated for all measurement areas, which shows a sharp maximum in the position: $r_1 = 0.0$, $r_2 = 0.0$, $r_3 = 0.0$ (Fig. 6). This maximum can be approximated by the following low-index crystallographic relationship:

$$(0\,0\,1)\mathrm{W} \| (0\,0\,0\,1)\mathrm{Al_2O_3}$$
$$[1\,0\,0]\mathrm{W} \| [1\,1\,\bar{2}\,0]\mathrm{Al_2O_3}.$$

The scattering around the dominant crystallographic relationship can be described by the rotation around the axis perpendicular to the basal planes by angles up to 2°. This relationship corresponds, depending on the measurement field, to 6–10% of the total W/Al_2O_3 interphase boundary length. Other relations are randomly distributed in rotation space. In this sense, the crystallographic relationship identified by means of TEM has a rather incidental character.

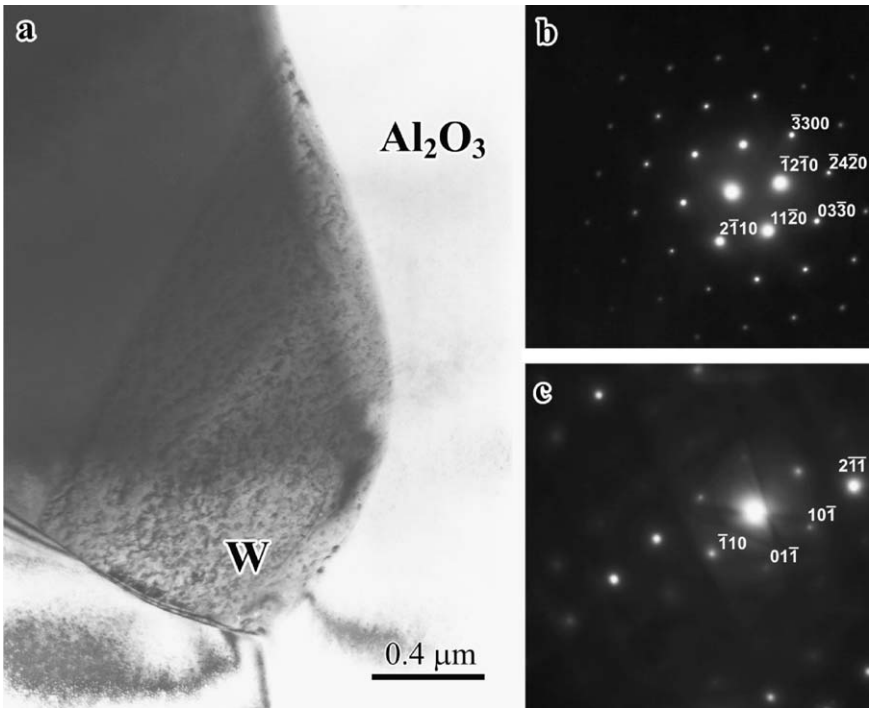

Fig. 4. Microstructure of Al_2O_3/W composite obtained by TEM. (a) Bright field image; (b) SAED from W grain; (c) SAED from Al_2O_3 grain.

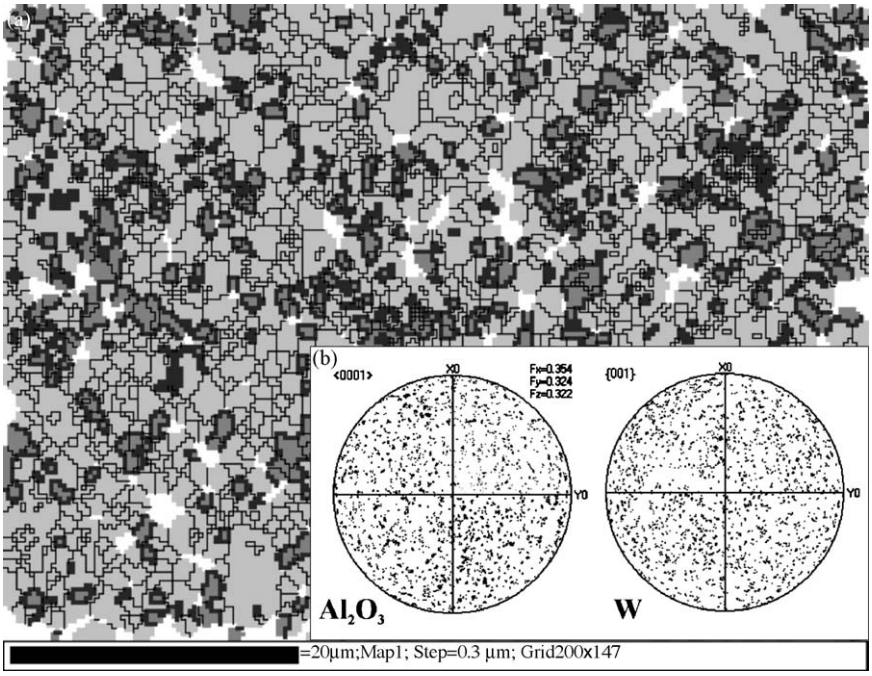

Fig. 5. Microstructure of Al_2O_3/W composite. (a) ESEM/EBSD orientation map; Al_2O_3 grains: light grey; W grains: dark grey; white regions: not indexed; thick lines: Al_2O_3/W interphase boundaries, thin lines: grain boundaries. (b) Stereographic projections of directions $\langle 0\,0\,0\,1\rangle$ in Al_2O_3 grains and $\langle 0\,0\,1\rangle$ in W grains, respectively; the measurement field as in (a).

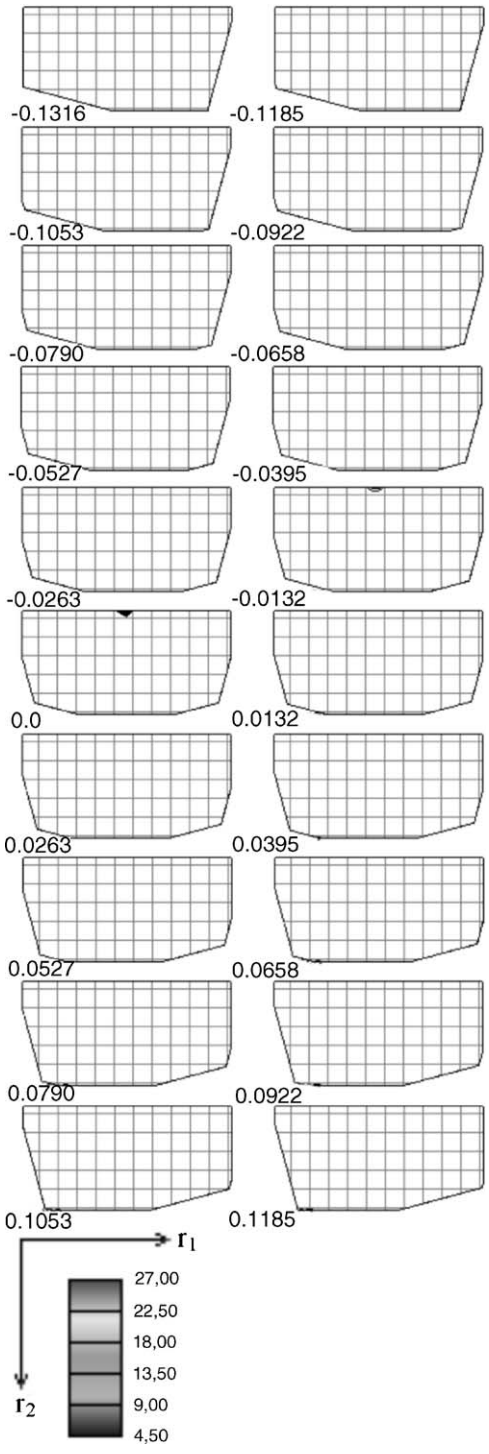

Fig. 6. Misorientation Distribution Function between Al_2O_3 and W grains; Rodrigues' representation $r_1 \in [-1, 1]$, $r_2 \in [0, 1]$, $r_2 \in [-0.131652, 0.118487]$, cross-section $r_3 = \text{const.}$, asymmetric domain (T_d, D_3).

3. Conclusions

- For quantitative characterization of interphase boundaries between the matrix-inclusion in composites: Al_2O_3/WC and Al_2O_3/W, large sets of crystallographic misorientations data were used. Each misorientation value was calculated from two orientations measured by an EBSD/ESEM technique in neighbouring areas of different phases. For two arrangements of crystallite symmetries (D_3–D_6 in Al_2O_3/WC and D_3–T_d in Al_2O_3/W), the MDFs were constructed by representing each physically distinct misorientation only once.
- The examples of MDFs calculated for the Al_2O_3/WC and Al_2O_3/W composites showed that certain crystallographic relationships between WC and Al_2O_3 as well as between W and Al_2O_3 were not random and some of them appear much more frequently than the others. The highest frequencies were observed for the crystallographic relationships:

$$\begin{matrix}(0\,0\,0\,1)\mathrm{WC}\,||\,(0\,0\,0\,1)\mathrm{Al_2O_3} \\ [1\,1\,\bar{2}\,0]\mathrm{WC}\,\|\,[1\,0\,\bar{1}\,0]\mathrm{Al_2O_3}\end{matrix},$$

$$\begin{matrix}(2\,\bar{1}\,\bar{1}\,0)\mathrm{WC}\,\|\,(2\,\bar{1}\,\bar{1}\,0)\mathrm{Al_2O_3} \\ [0\,0\,0\,\bar{1}]\mathrm{WC}\,\|\,[0\,1\,\bar{1}\,0]\mathrm{Al_2O_3}\end{matrix}$$

and

$$\begin{matrix}(0\,0\,1)\mathrm{W}\,||\,(0\,0\,0\,1)\mathrm{Al_2O_3} \\ [1\,0\,0]\mathrm{W}\,||\,[1\,1\,\bar{2}\,0]\mathrm{Al_2O_3}\end{matrix}.$$

Acknowledgements

Financial support from the Polish Committee for Scientific Research (KBN), contract No. 4 T08D 010 25 is gratefully acknowledged.

Appendix A. Description of boundary misorientation

The grain boundary geometry is definite if the boundary plane orientation (two degrees of freedom) and the rotation between two misoriented crystal lattices (three degrees of freedom) are known. The topography of orientations in selected sample planes can be obtained by well-developed OM techniques. Thus, it becomes relatively easy to obtain the characteristics of misorientations between neighbouring areas. To gain information on the boundary plane position requires more tedious topography measurements of orientations in successive sample layers[7] and this is possible with the help of Focused Ion Beam (FIB) technique. However, the information contained in the misorientation between neighbouring grains is frequently sufficient to determine the basic boundary features. The misorientation between crystallites A and B is defined as rotation Γ_{AB} transforming the crystallite B reference system into crystallite A reference system: $K_A = \Gamma_{AB} \cdot K_B$. The misorientation may be described mathematically in several ways. The natural is the description by the axis/angle pair. We can always find the axis of rotation around that which transforms the one crystallite into the second. For the rotation description, we can also use the rotation matrix, the Euler angles, the Rodrigues vector and the quaternion. Each representation may have advantages for certain situations.

Due to the crystallographic symmetry, the misorientation description is not unequivocal. Symmetrically equivalent representations of Γ^{e}_{AB} misorientation are given by the formula: $\Gamma^{e}_{AB} = S_i \cdot \Gamma_{AB} \cdot P_j$, ($i = 1, \ldots, M$, $j = 1, \ldots, N$), where S_i and P_j are symmetry elements of the first and second crystallite, respectively. So, the misorientation is described by $N{\cdot}M$ symmetrically equivalent variants, distributed in the whole of rotational space. For quantitative analysis of interfaces, the misorientation should be unique. It can be made so only if a part of the rotational space is considered. The part in question, called the asymmetric domain, is constructed by representing each physically distinct misorientation only once (e.g.[8]). To characterize interphase boundary between matrix-inclusion in composites, we have chosen Rodrigues' representation, which is unique and possesses certain properties of rectilinearity that make it relatively easy to construct asymmetric domains for different arrangements of crystallite symmetries. Following Frank,[9] we define the Rodrigues' parameters as follows: $r_1 = x_v \cdot tg(\omega/2)$, $r_2 = y_v \cdot tg(\omega/2)$, $r_2 = z_v \cdot tg(\omega/2)$ where ω is the rotation angle, x_v, y_v, z_v are the rotation axis vectors.

The misorientation is calculated from two orientations measured in the neighbouring sample areas of different phases. The list of all orientation pairs measured on both sides of the inclusion-matrix boundary is determined on the basis of the measured orientation topography. The number of pairs is proportional to the total length of interphase boundaries in the measurement field. The set of single misorientations is used to calculate the MDF.[10] The next step assumes the identification of the MDF maxima, followed by their crystallographic interpretation. When the misorientation and the parameters of unit cells of both neighbouring crystallites are known, the crystallographic relationships between them can be described with the pairs of parallel crystallographic planes and the pairs of parallel crystallographic directions lying in these planes:

$$r_1, r_2, r_3 \rightarrow \begin{matrix} (h_A k_A l_A)||(h_B k_B l_B) \\ [u_A v_A w_A]||[u_B v_B w_B] \end{matrix}.$$

References

1. Pędzich, Z., Haberko, K., Faryna, M. and Sztwiertnia, K., Mechanical properties and crystallographic orientation characteristics of selected particulate composites. *Polish Ceramic Bulletin*, Polish Academy of Sciences, 2002, 146–152.
2. Pędzich, Z. and Faryna, M., Fracture and crystallographic phase correlation in alumina base particulate composites. *Key Eng. Mater.*, 2005, **290**, 142–148.
3. Dingley, D. J., On-line determination of crystal orientation and texture determination in an SEM. *Proc. Royal Microsc. Soc.*, 1984, **19**, 74–75.
4. Fundenberger, J. J., Morawiec, A., Bouzy, E. and Lecomte, J. S., Polycrystal orientation maps from TEM. *Ultramicroscopy*, 2003, **96**, 127–137.
5. Kronberg, M. L., Plastic deformation of single crystals of sapphire: basal slip and twinning. *Acta Mater.*, 1957, **5**, 507–527.
6. Faryna, M., Microbeam studies of alumina-based composite. *Arch. Metall. Mater.*, 2006, **51**, 75–81.
7. Saylor, D. M., Morawiec, A. and Rohrer, G. S., Distribution of grain boundaries in magnesia as a function of five macroscopic parameters. *Acta Mater.*, 2003, **51**, 3663–3674.
8. Morawiec, A., *Orientations and Rotations*. Springer Verlag, Berlin, 2003.
9. Frank, F. C., Orientation mapping. *Metall. Trans. A*, 1987, **19A**, 403–408.
10. Pospiech, J., Sztwiertnia, K. and Haessner, F., The misorientation distribution function. *Texture Microstruct.*, 1986, **6**, 201–215.